Volume 1 | Number 1 | Jan 2013 | Pages 1–100

Journal of
Materials Chemistry A

Materials for energy and sustainability
www.rsc.org/materialsA

ROYAL SOCIETY
OF CHEMISTRY

ROYAL SOCIETY
OF CHEMISTRY

www.rsc.org/materialsA

Journal Name

Journal of Materials Chemistry A

Dynamic Article Links ▶

ARTICLE TYPE

Synthesis of amorphous cobalt sulfide polyhedral nanocages for high performance supercapacitors

Zhen Jiang,[a] Weijun Lu,[a] Zhengping Li,[a] Kuan Hung Ho[b], Xu Li[c], Xiuling Jiao,*[a] and Dairong Chen*[a]

Amorphous cobalt sulfide polyhedral nanocages are synthesized by utilizing zeolitic imidazolate framework-67 (ZIF-67) nanocrystals as the templates. And electrochemical characterization shows that the CoS nanocages exhibit high
10 **specific capacitance, owing to its amorphous phase and novel structure.**

With the increasing demand for power and energy in the application of hybrid electric vehicles and modern portable electronic devices, novel electrode materials for advanced energy
15 storage devices are urgently desired.[1-3] Supercapacitors, also known as electrochemical capacitors (ECs), have gained much attention as promising energy storage devices due to their attractive properties, including high power density, fast charge and recharge capability, excellent reversibility and long cycle
20 life.[4,5] In order to improve ECs' energy densities, numerous efforts have been devoted to developing the novel electrode materials with high performances. It should be noted that enormous progress in nanoscience and nanotechnology has also accelerated the exploration of new electrode structures such as
25 morphology, size, porosity and so forth, which may significantly enhance the utilization of active materials and shorten the transport path of ion and electron.[6-10]

Metal sulfides are typical pseudocapacitive materials that can achieve relative high capacitance.[11-14] As an important class of
30 metal sulfides, cobalt sulfides have been employed as electroactive materials for high-performance electrochemical capacitive energy storage applications.[15-18, 40, 42-44] It has been accepted that the performance of one material highly depends on its morphology.[19-21] In the design of EC electrode materials, high
35 specific surface area and suitable pore-size distribution are two important factors which should be considered.[22] Hollow nanostructures are usually fabricated to increase the surface area of the materials and hollow spheres with various components have been widely reported.[23-25] And the anisotropic morphologies
40 and high-curvature surfaces of non-spherical structures have impact on their properties, which may bring new applications. However, reports about hollow structures with non-spherical morphology are still not much.[26-28] Zeolitic imidazolate framework (ZIF) as a classic example of metal-organic
45 framework (MOF) displays exceptionally high thermal stability and chemical robustness, and can be employed as an ideal template to prepare hollow nanostructures.[29,30,37] Additionally, the pseudocapacitance of materials is also related to the

crystallinity.[22,31-33] A well crystallized structure has difficulty in
50 expanding or contracting, limiting the permeation and diffusion of ions. On the contrary, the continuous redox reaction of an amorphous composite occurs not only on the surface but also in the bulk of the powder, leading to better performance compared with crystallized structures.

55 Herein, a facile and efficient route to the amorphous CoS hollow polyhedra by utilizing ZIF-67 nanocrystals as the templates is reported (Fig. 1). In this work, the CoS nanocages exhibit superior pseudocapacitance property.
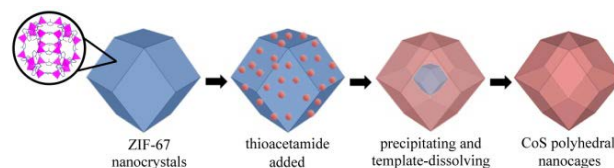

60 **Fig. 1** The formation illustration of CoS polyhedral nanocages.

ZIF-67 templates were fabricated by mixing the cobalt nitrate and 2-methylimidazole in methanol with the mixture being aged at ambient conditions for 24 h. The X-ray diffraction (XRD) pattern matches well with the simulated as well as the published
65 pattern (Fig. S1a), demonstrating that the as-synthesized templates are phase-pure. The shape of ZIF-67 is rhombic dodecahedron, which is the same as that of ZIF-67 nanocrystals in previous reports, as shown in the field-emission scanning electron microscopy (FE-SEM) and transmission electron
70 microscopy (TEM) images (Fig. S1b-d). Also the products exhibit a remarkably narrow size distribution with an average particle size of ca. 900 nm.

The CoS nanocages were fabricated with rhombic dodecahedral ZIF-67 as both template and cobalt precursor, and
75 thioacetamide as sulfur precursor. The reactants were refluxed for 1 h, using ethylene glycol as solvent. The XRD pattern presented in Fig. 2b shows a weak broad peak around 23 °, demonstrating the amorphous nature of the as synthesized cobalt sulfide sample. It is similar to the previous reports that amorphous cobalt sulfide
80 was obtained in ethylene glycol solvent.[34] And from the EDS pattern (Fig. 2a), the atomic ratio of Co:S is approximately about 1:1.17 .

Panoramic views from the SEM image (Fig. 2c) show that the sample consists of uniform nanocages without impurity. The
85 nanocages well inherits the morphology and dimension of the ZIF-67 templates from magnified SEM image (Fig. 2d). And the

rough shell is composed of small particles. Their interior space can be examined directly by SEM image for cracked nanocages (Fig. 2e). From the TEM images (Fig. 2f, g), the inner cavity is clearly revealed by the contrast between the shells and hollow 5 interiors. And the thickness for the shell is around 60 nm (inset in Fig. 2g).
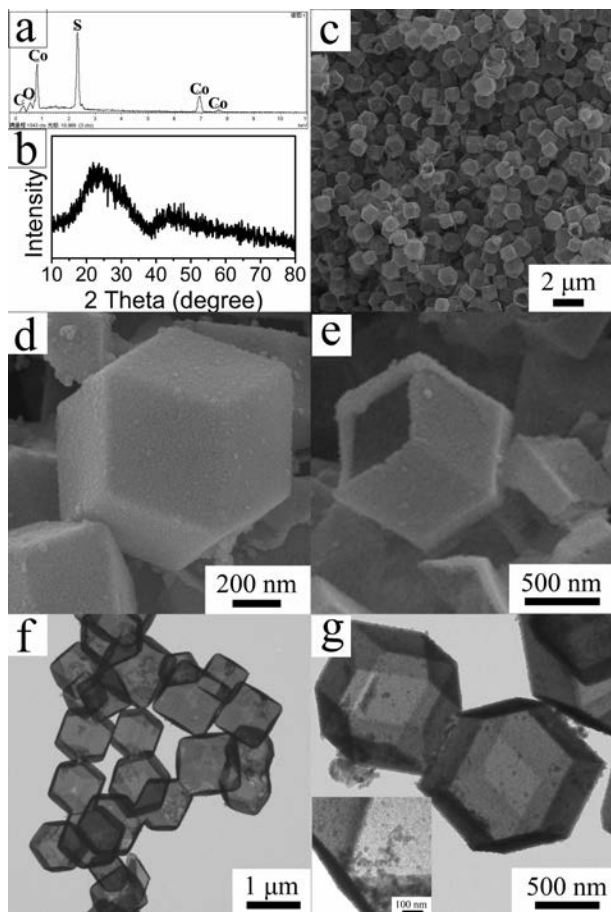

Fig. 2 EDS (a) and XRD (b) patterns, SEM (c-e) and TEM (f, g) images of the nanocages.

10   The possible formation mechanism is proposed as follows. At first, S^{2-} anions hydrolyzing from thioacetamide reacts with the Co^{2+} cations slowly dissolving from the surface of ZIF-67 templates, resulting in cobalt sulfide nanoparticles around the templates (Fig. S2a, b). As the reaction going on, a gap is 15 gradually formed between the ZIF-67 core and the cobalt sulfide shell (Fig. S2c, d). At last, the ZIF-67 cores are completely consumed, and well-defined hollow truncated rhombic dodecahedral nanocages are formed. The precise control of the S^{2-} hydrolyzing and ZIF-67 template dissolving is crucial for 20 fabricating high-quality CoS nanocages in this strategy. Excessively fast hydrolysis causes inevitable formation of abundant disordered impurities in solution and incapably induces formation of hollow structures by heterogeneous nucleation. As shown in Fig. S3a, nanoparticles formed when the hydrolysis rate 25 of S^{2-} anion is much too high. On the contrary, the low hydrolysis rate of S^{2-} anion can not ensure the sufficient S^{2-} at the beginning of the reaction. Therefore, the templates have been dissolved partially and can not remain the polyhedral morphology when the S^{2-} anion reacts on the surface of templates. Eventually, the

30 irregular hollow structures formed, with thinner shell (ca. 17 nm) and looser particles aggregation (inset in Fig. S3b).

    Both the surface area and pore-size distribution are important for the electroactive materials in supercapacitor applications. Therefore, the nanocages were investigated for their surface area 35 and porosity property by N_2-adsorption/desorption measurement, with the irregular hollow structures and nanoparticles above (Fig. S3) as references. As shown in Fig. S4, IV-type isotherms with H3-type hysteresis loops indicate the presence of mesopores in the three samples. It is commonly attributed to particle aggregates 40 with slit-shaped pores. Compared with the other two samples, the nanocages give a relatively concentrated mesopore distribution in the size of 3-5 nm (Fig. S4b). It was reported that the pore-size distribution within 2-5 nm is favor for the behavior of supercapacitors,[35,36] which will be further discussed in the next 45 section. The surface areas of the two hollow structures are 96.3 $m^2 \cdot g^{-1}$ (CoS nanocages) and 103.4 $m^2 \cdot g^{-1}$ (the irregular hollow structures), much larger than the CoS individual particles (33.1 $m^2 \cdot g^{-1}$).
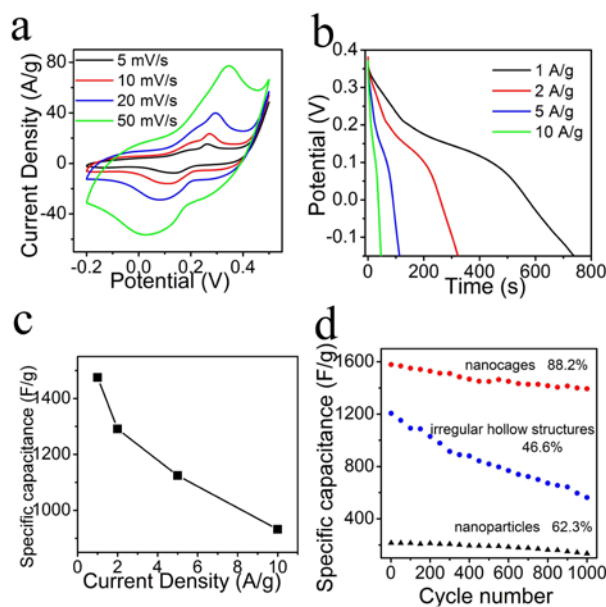

50 **Fig. 3** (a) CV curves of the nanocages at various scan rates ranged from 5 to 50 $mV \cdot s^{-1}$, (b) discharge voltage curves at various current densities ranged from 1 to 10 $A \cdot g^{-1}$, (c) specific capacitance calculated from the discharge voltage curves, (d) cycling performance of the nanocages, irregular hollow structures and individual nanoparticles.

55   Electrochemical measurements were conducted in a three-electrode cell to explore the electrochemical properties of the CoS nanocages as pseudo-capacitor electrode materials. Fig. 3a shows the typical CV curves of the CoS nanocages, the irregular hollow structures and the nanoparticles in a 1.0 M KOH aqueous 60 electrolyte at a scan rate of 10 $mV \cdot s^{-1}$. The mechanism of electrochemical redox of cobalt sulfide can be speculated according to that of $Co(OH)_2$ in alkaline electrolyte, as shown in eq. (1) and (2).[15, 16, 41]

$$CoS + OH^- \rightleftharpoons CoSOH + e^- \qquad (1)$$
65 $$CoSOH + OH^- \rightleftharpoons CoSO + H_2O + e^- \qquad (2)$$
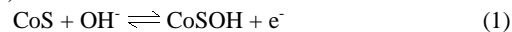
    The specific capacitances of the two hollow structures calculated from CV curves are higher than that of the individual particles (Fig. S3c). This outstanding electrochemical

performance are mainly attributed to the hollow nanostructure with large surface area, increasing the amount of electroactive sites, boosting the electrical conductivity and facilitating transport of the electrolyte.[9,38,39] Moreover, the abundant mesopores in the structure can serve as ion reservoirs, which might diminish the diffusion distance to the interior surfaces and accelerate the process of the ion diffusion in the electrode, so as to enhance the electrochemical property. Therefore, the nanocages with more appropriate mesopore size distribution present higher specific capacitance than the irregular hollow structure.

To further evaluate the application potential of the CoS nanocages, the CV test and galvanostatic charge/discharge were carried out in 1.0 M KOH aqueous electrolyte. Fig. 3b shows the CV curves of the CoS nanocages at different scan rates ranged from 5 to 50 $mV \cdot s^{-1}$. The specific capacitance of the CoS nanocages calculated from the CV curve is 1812 $F \cdot g^{-1}$ at a scan rate of 5 $mV \cdot s^{-1}$ and 1201 $F \cdot g^{-1}$ at a high scan rate of 50 $mV \cdot s^{-1}$. Fig. 3c shows the galvanostatic discharge curves of the CoS nanocages at different current densities ranged from 1 to 10 $A \cdot g^{-1}$. From the curve, the specific capacitance is 1475 $F \cdot g^{-1}$ at a discharge current density of 1 $A \cdot g^{-1}$. And at a relatively high current density of 10 $A \cdot g^{-1}$, a specific capacitance of 932 $F \cdot g^{-1}$ is obtained. The cycling performance of the CoS nanocages electrode was also evaluated by galvanostatic charge-discharge tests for 1000 cycles at the current density of 10 $A \cdot g^{-1}$ and compared with that of the irregular hollow structures and nanoparticles under the same condition (Fig. 3d). After 1000 cycles, the specific capacitance of the nanocages remains ca. 88.2%, demonstrating the long-term electrochemical stability of the CoS nanocages. Even after 3000 cycles, the specific capacitance still remains ca. 70.3% (Fig. S5). As a comparison, the irregular hollow structures and nanoparticles show 46.6% and 62.3% maintained after 1000 cycles. The worse cycling stability of the CoS individual particles possibly results from the compact particles which hinder electrolyte transport and active site accessibility during the cycling process. Compared with the nanocages, the worst cycling stability of the irregular hollow structures is probably due to the collapse during the redox reaction. From the TEM images of the nanocages and the irregular hollow structures after cycling test (Fig. S6), the morphology of the nanocages still retained while the irregular hollow structures became nanoparticles almost. Smaller particles which compose looser shell may easily dissolve and draw off during the continuous redox reaction, leading to the collapse of the irregular hollow structures and the great decrease of the specific capacitance. To evaluate the practical performance of the electrode in a full-cell setup, a cobalt sulfide nanocage-active carbon-based asymmetric capacitor was fabricated in our study. On the basis of the SC values and potential ranges for the cobalt sulfide nanocages and active carbon, the mass ratio between positive and negative electrodes is optimized (see methods in †ESI, Fig. S7). Fig. S8 shows the galvanostatic charging/discharging curves of the asymmetric capacitor at various current densities in the potential range from 0 to 1.5 V. The specific capacitance is 104 $F \cdot g^{-1}$ at 1 $A \cdot g^{-1}$. Therefore, it is very likely that the device capacitance can be further increased by improving the capacitance of the negative active carbon electrode. The Ragone plot (Fig. S8c) relates the energy density to the power density of the asymmetric capacitor. The energy density of the supercapacitors decreases from 32.5 to 23.3 $Wh \cdot kg^{-1}$ as the power density increases from 0.75 to 6.01 $kW \cdot kg^{-1}$. In brief, the novel structure of CoS nanocages brings about better performance as a pseudo-capacitor electrode. And the relation between the structures and properties is worth deeply investigating in the future.

In summary, amorphous cobalt sulfide polyhedral nanocages have been fabricated by utilizing ZIF-67 nanocrystals as the templates. The precise control of the S^{2-} hydrolyzing and ZIF-67 template dissolving is crucial for fabricating high-quality CoS nanocages. Electrochemical characterization shows that the CoS nanocages exhibit high specific capacitance, owing to its amorphous phase and novel structures.

Acknowledgements

Notes and references

[a]*Key Laboratory for Special Functional Aggregate Materials of Education Ministry, School of Chemistry & Chemical Engineering, Shandong University, Jinan, 250100, China. Fax: +86-531-88364281; Tel: +86-531-88364280; E-mail: cdr@sdu.edu.cn*
[b]*Department of Materials Science and Engineering, National University of Singapore, Singapore 117574, Singapore;*
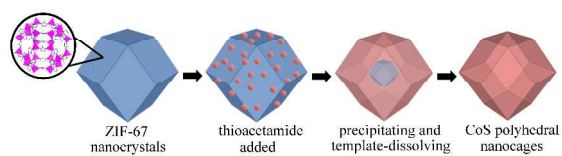[c]*Institute of Materials Research and Engineering (IMRE), Singapore 117602, Singapore*
† Electronic Supplementary Information (ESI) available: experimental details,XRD, TEM, SEM images. See DOI: 10.1039/b000000x/

1   A. S. Arico, P. Bruce, B. Scrosati, J. M. Tarascon and W. van Schalkwijk, *Nat. Mater.*, 2005, **4**, 366-377.
2   P. Simon and Y. Gogotsi, *Nat. Mater.*, 2008, **7**, 845-854.
3   M. Winter and R. J. Brodd, *Chem. Rev.*, 2004, **104**, 4245-4270.
4   J. Jiang, J. Liu, W. Zhou, J. Zhu, X. Huang, X. Qi, H. Zhang and T. Yu, *Energy Environ. Sci.*, 2011, **4**, 5000-5007.
5   J. R. Miller and P. Simon, *Science*, 2008, **321**, 651-652.
6   R. B. Rakhi, W. Chen, D. Cha and H. N. Alshareef, *Nano Lett.*, 2012, **12**, 2559-2567.
7   C. Shang, S. Dong, S. Wang, D. Xiao, P. Han, X. Wang, L. Gu and G. Cui, *ACS Nano*, 2013, **7**, 5430-5436.
8   Z. Yu, B. Duong, D. Abbitt and J. Thomas, *Adv. Mater.*, 2013, **25**, 3302-3306.
9   G. Zhang, H. Wu, H. E. Hoster, M. B. Chan-Park and X. Lou, *Energy Environ. Sci.*, 2012, **5**, 9453-9456..
10 X. Zhao, B. M. Sanchez, P. J. Dobson and P. S. Grant, *Nanoscale*, 2011, **3**, 839-855.
11 S. Peng, L. Li, C. Li, H. Tan, R. Cai, H. Yu, S. Mhaisalkar, M. Srinivasan, S. Ramakrishna, Q. Yan, *Chem. Commun.*, 2013, **49**, 10178-10180.
12 Z. Xing, Q. Chu, X. Ren, J. Tian, A. M. Asiri, K. A. Alamry, A. O. Al-Youbi and X. Sun, *Electrochem. Commun.*, 2013, **32**, 9-13.
13 C. Yuan, B. Gao, L. Su, L. Chen and X. Zhang, *J. Electrochem. Soc.*, 2009, **156**, A199-A203.
14 W. Zhou, X. Cao, Z. Zeng, W. Shi, Y. Zhu, Q. Yan, H. Liu, J. Wang and H. Zhang, *Energy Environ. Sci.*, 2013, **6**, 2216-2221.
15 B. Qu, Y. Chen, M. Zhang, L. Hu, D. Lei, B. Lu, Q. Li, Y. Wang, L. Chen and T. Wang, *Nanoscale*, 2012, **4**, 7810-7816.
16 F. Tao, Y. Zhao, G. Zhang and H. Li, *Electrochem. Commun.*, 2007, **9**, 1282-1287.
17 B. Wang, J. Park, D. Su, C. Wang, H. Ahn and G. Wang, *J. Mater. Chem.*, 2012, **22**, 15750-15756.

18 L. Zhang, H. Wu and X. Lou, *Chem. Commun.*, 2012, **48**, 6912-6914.

19 C. Kuo, Y. Chu, Y. Song and M. Huang, *Adv. Funct. Mater.*, 2011, **21**, 792-797.

20 J. Nai, S. Wang, Y. Bai and L. Guo, *Small*, 2013, **9**, 3147-3152.

21 Z. Wang and X. Lou, *Adv. Mater.*, 2012, **24**, 4124-4129.

22 G. Wang, L. Zhang and J. Zhang, *Chem. Soc. Rev.*, 2012, **41**, 797-828.

23 S. Kim, M. Kim, W. Lee and T. Hyeon, *J. Am. Chem. Soc.*, 2002, **124**, 7642-7643.

24 Q. Peng, Y. Dong and Y. Li, *Angew. Chem. Int. Ed.*, 2003, **42**, 3027-3030.

25 C. I. Zoldesi and A. Imhof, *Adv. Mater.*, 2005, **17**, 924-928.

26 Y. Liu, J. Goebl and Y. Yin, *Chem. Soc. Rev.*, 2013, **42**, 2610-2653.

27 S. E. Skrabalak, L. Au, X. Li and Y. Xia, *Nat. Protocols*, 2007, **2**, 2182-2190.

28 Z. Wang, D. Luan, C. Li, F. Su, S. Madhavi, F. Y. C. Boey and X. Lou, *J. Am. Chem. Soc.*, 2010, **132**, 16271-16277.

29 K. E. deKrafft, C. Wang and W. Lin, *Adv. Mater.*, 2012, **24**, 2014-2018.

30 Z. Jiang, H. Sun, Z. Qin, X. Jiao and D. Chen, *Chem. Commun.*, 2012, **48**, 3620-3622.

31 Z. Wang, Z. Wang, W. Liu, W. Xiao and X. Lou, *Energy Environ. Sci.*, 2013, 87-91.

32 J. Zheng, P. Cygan and T. Jow, *J. Electrochem. Soc.*, 1995, **142**, 2699-2703.

33 J. P. Zheng and Y. Xin, *J. Power Sources*, 2002, **110**, 86-90.

34 D. Song, Q. Wang, Y. Wang, Y. Wang, Y. Han, L. Li, G. Liu, L. Jiao and H. Yuan, *J. Power Sources*, 2010, **195**, 7462-7465.

35 G. Zhang and X. Lou, *Adv. Mater.*, 2013, **25**, 976-979.

36 H. Zhou, D. Li, M. Hibino and I. Honma, *Angew. Chem. Int. Ed.*, 2005, **44**, 797-802.

37 Z. Jiang, Z. Li, Z. Qin, H. Sun, X. Jiao and D. Chen, *Nanoscale*, 2013, **5**, 11770-11775.

38 J. Han, Y. Dou, J. Zhao, M. Wei, D. G. Evans and X. Duan, *Small*, 2013, **9**, 98-106.

39 M. Shao, F. Ning, Y. Zhao, J. Zhao, M. Wei, D. G. Evans and X. Duan, *Chem. Mater.*, 2012, **24**, 1192-1197.

40 Z. Yang, C. Chen and H. Chang, *J. Power Sources*, 2011, **196**, 7874-7877.

41 L. Cao, F. Xu, Y. Liang and H. Li, *Adv. Mater.*, 2004, **16**, 1853-1857.

42 C. Chen, Z. Shih, Z. Yang, H. Chang, *J. Power Sources*, 2012, **215**, 43-47.

43 J. Pu, Z. Wang, K. Wu, N. Yu, E. Sheng, *Phys, Chem. Chem. Phys.*, 2014, **16**, 785-791.

44 H. Wan, X. Ji, J. Jiang, J. Yu, L. Miao, L. Zhang, S. Bie, H. Chen, Y. Ruan, *J. Power Sources*, 2013, **243**, 396-402.

Table of contents

ZIF-67 nanocrystals → thioacetamide added → precipitating and template-dissolving → CoS polyhedral nanocages

Amorphous cobalt sulfide polyhedral nanocages are synthesized by utilizing zeolitic imidazolate framework-67 (ZIF-67) nanocrystals as the templates.